Structure of silver iodide/silver selenate fast-ion-conducting glasses: neutron diffraction experiments

1998 J. Phys.: Condens. Matter 10 6229

(http://iopscience.iop.org/0953-8984/10/28/005)

J. Phys.: Condens. Matter **10** (1998) 6229–6242. Printed in the UK PII: S0953-8984(98)91569-7

Structure of silver iodide/silver selenate fast-ion-conducting glasses: neutron diffraction experiments

Cornelia Cramer†, D L Price‡ and Marie-Louise Saboungi‡

† Institut für Physikalische Chemie, Universität Münster, D-48149 Münster, Germany
‡ Argonne National Laboratory, Argonne, IL 60439, USA

Received 12 February 1998, in final form 29 April 1998

Abstract. Structure factors, $S(Q)$, of many fast-ion-conducting glasses show peaks at very low momentum-transfer values, $\hbar Q$, which can be attributed to a characteristic intermediate-range order. We report on a neutron diffraction study of the fast-ion-conducting glass-forming system $x(\mathrm{AgI})_2{\cdot}(1-x)\mathrm{Ag_2SeO_4}$ with $x \approx 0.5$ in the glassy, partly crystallized, and liquid states. The structure factors of the glass and the melt are similar: the very-low-Q peak (VLQP) at $Q \approx 0.75$ Å^{-1} survives the melting process and shifts towards higher Q-values with increasing temperature. The partly crystallized glasses show Bragg peaks at around 0.8 Å^{-1}, whereas no intensity in this Q-range has been observed for crystalline silver selenate. In the glasses, the intensity of the VLQP increases with AgI content and its position shifts towards lower Q. The origin of this peak is discussed. The peaks observed in $S(Q)$ are assigned to various ionic species, and coordination numbers for these species, are derived from the total pair correlation functions, $T(r)$.

1. Introduction

Among the fast-ion-conducting glasses, glasses containing AgI show the highest dc conductivities (10^{-2} Ω^{-1} cm^{-1} at ambient temperature), of the same order as those of aqueous ionic solutions. Contrary to crystalline-ion conductors, the composition—and thereby the physical properties—of the glasses can be easily changed, making them interesting materials for application in batteries and sensors. However, many of their physical properties are not yet understood. Some outstanding questions are:

(i) How does the ion dynamics relate to the glass structure?
(ii) Does a biphasic structure with AgI-rich regions exist?

Speculations on the formation of AgI clusters have been advanced based on the observation that the structure factor, $S(Q)$, shows for many of these glasses a peak at very low momentum-transfer values $\hbar Q$, typically at $Q \approx 0.8$ Å^{-1} as first reported for an AgI-containing phosphate glass [1], and later for AgI-containing borate glasses [2]. Since then, many fast-ion-conducting glasses have been probed for the existence of such peaks (see, e.g., [1–9]).

In the literature, the peak occurring at very low Q has been termed either the 'first sharp diffraction peak', Q_F (FSDP) [2], or the 'pre-peak', Q_P [1, 3, 9]. However, the term FSDP is generally used in connection with intermediate-range order (IRO) in glasses and liquids where the relationship $Q_F r_1 \approx 2.5$ holds, r_1 being the nearest-neighbour distance [10, 11]. In addition, it has been shown that, in these cases, the structure factors show

0953-8984/98/286229+14$19.50

a striking similarity when scaled as a function of Qr_1 [12, 13]. The term 'pre-peak' is generally applied in connection with chemical ordering in glasses with two metallic species [14] where $Q_P r_1$ ranges from 4.3 to 5.0. In many fast-ion-conducting glasses, the first peak appears at $Q_1 < 1$ Å^{-1}, corresponding to values of $Q_1 r_1$ ranging from 1 to 1.3. We propose a different term, the 'very-low-Q peak' (VLQP), to designate this new feature. An overview of the various types of peak for disordered materials is given elsewhere [15].

Strong peaks in $S(Q)$ give rise to pronounced oscillations in the pair distribution function, $g(r)$, and so peaks at $Q_1 \approx 0.8$ Å^{-1} can be attributed to correlations between entities which occur on a length scale of $d_1 \approx 2\pi/Q_1 \approx 8$ Å, reflecting IRO. Order in glasses has frequently been investigated using a variety of experimental methods. New results obtained by means of neutron and x-ray diffraction are, for example, presented in [16–18]. The appearance of the VLQP in halide-doped glasses was first interpreted in terms of small microcrystalline AgI clusters, with a structure similar to that of the high-temperature phase of AgI, α-AgI [1, 2], distributed in a glassy host matrix. Using reverse Monte Carlo (RMC) simulations based on neutron and x-ray diffraction data for phosphate [5, 6], borate [7], and molybdate and tungstate glasses [8], Börjesson *et al* calculated partial structure factors which confirmed that in no case does the VLQP originate from AgI clusters. Recently, Rousselot *et al* [9] attributed the VLQP to a formation of clusters of favourable ionic sites which also occurs in ion-conducting glasses that do *not* contain AgI.

In the present work, we focus on an ionic glass consisting of discrete Ag^+, I^-, and SeO_4^{2-} ions. Neither AgI nor Ag_2SeO_4 themselves form glasses, but mixtures in a limited concentration range can be readily quenched [19–22] to glasses with remarkably low glass transition temperatures, T_g, ranging from 350 K to 295 K [20, 22]. At temperatures about 30 K above T_g, the glasses tend to crystallize, and the conductivity drops by about an order of magnitude [23]. Dynamic conductivity spectra which range from a few Hz to the THz regime have been reported for $x(AgI)_2 \cdot (1-x)Ag_2SeO_4$ [24]. The interpretation of these conductivity spectra includes the idea of different 'target sites' that the mobile silver ions might hop into. However, more structural investigations are needed to link the 'favourable' and 'unfavourable' sites deduced from the conductivity spectra to the actual glass structure found in silver selenate glasses.

In this paper, we report on neutron diffraction results on fast-ion-conducting glasses with the compositions $x(AgI)_2 \cdot (1-x)Ag_2SeO_4$ with $x = 0.40$, 0.48, and 0.54 and for crystalline silver selenate, c-Ag_2SeO_4. Note that this notation has been chosen so that both components contain equal amounts of silver ions. The temperature dependence of $S(Q)$ was studied for $x = 0.48$. A model of the structure based on that of crystalline silver selenate is proposed. We also discuss the existence of the VLQP in the glasses and show that it survives the melting process.

2. Experimental procedure

The glasses were synthesized in a darkroom under safelight. A greyish-white precipitate was produced by slowly adding the stoichiometric amount of selenic acid (95% solution) to an aqueous solution of silver nitrate, via the reaction

$$2AgNO_3(aq) + H_2SeO_4(aq) \longrightarrow Ag_2SeO_4 \downarrow + 2HNO_3(aq).$$

The x-ray diffraction pattern obtained for the precipitate was in perfect agreement with published data for Ag_2SeO_4 [25], and confirmed that a single-phase material was formed.

To produce a desired composition, corresponding amounts of AgI and Ag_2SeO_4 were thoroughly mixed, melted, and stirred in a quartz crucible at 320 °C for about one hour. No decomposition of the selenate could be detected. The glass samples were prepared by rapid quenching of the melt between thick non-corrosive metal plates. The light-sensitive glass samples were stored in dark containers and kept in a refrigerator because of their strong tendency to crystallize at temperatures close to their very low T_g.

Time-of-flight neutron diffraction measurements were performed on GLAD at IPNS. For the ambient-temperature measurements, cylindrical vanadium containers were used. For the high-temperature runs, the sample was contained in a cylindrical sealed quartz tube. For $x = 0.48$, data were collected at 300 K, 335 K, 373 K, and 573 K, while for $x = 0.40$ and 0.54, and c-Ag_2SeO_4, spectra were recorded only at room temperature.

The background (with and without the furnace), a standard vanadium rod, and the empty tubes were measured at ambient temperature and 573 K. The data analysis followed standard procedures [26, 27] and included corrections for the background, the scattering from the containers, absorption, multiple scattering, inelasticity effects and incoherent scattering. The structure factors of $0.48(AgI)_2{\cdot}0.52Ag_2SeO_4$ at room temperature obtained by measurements in a vanadium container and in a quartz container within the furnace were in perfect agreement.

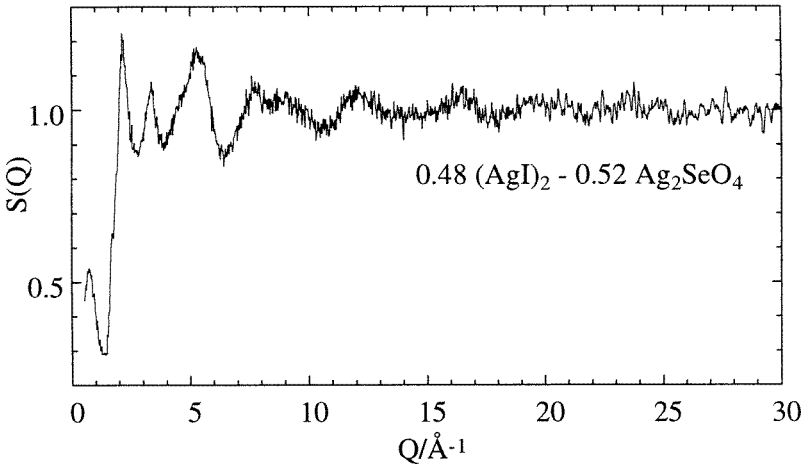

Figure 1. The structure factor at ambient temperature of $0.48(AgI)_2{\cdot}0.52Ag_2SeO_4$ glass.

3. Results and discussion

3.1. Reciprocal space: the structure factors, $S(Q)$

In this work, we have adopted the Faber–Ziman definition of the average structure factor as given by

$$S(Q) = \frac{1}{\langle b\rangle^2}\left[\sum_i \sum_j x_i x_j \langle b_i\rangle\langle b_j\rangle S_{ij}(Q)\right] \tag{1}$$

where $\langle b\rangle = \sum_i x_i b_i$. Here, x_i represents the atomic fraction of the ith element, b_i its coherent scattering length, and $S_{ij}(Q)$ is the partial structure factor for the (i, j) element

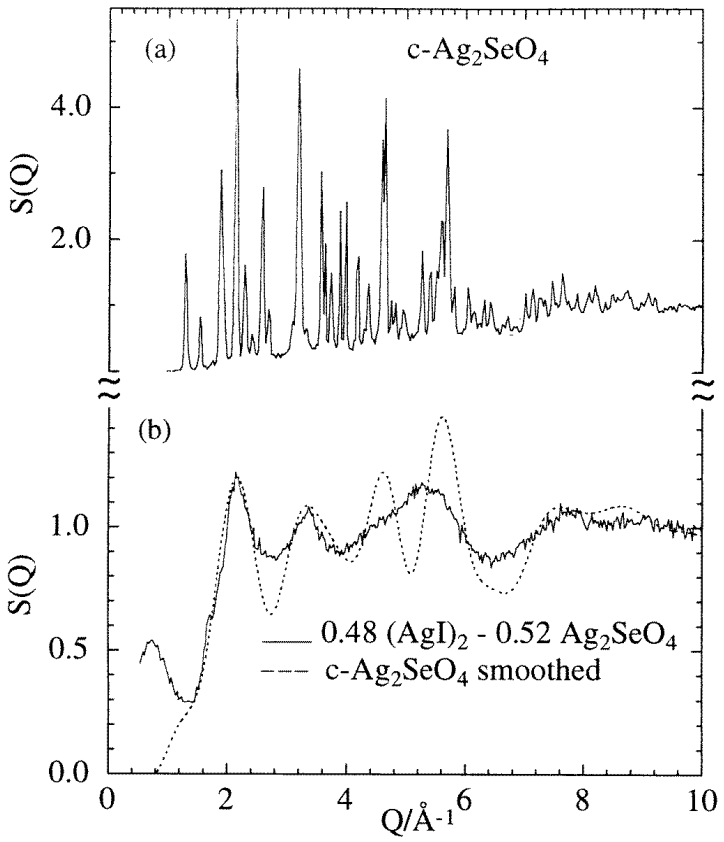

Figure 2. Structure factors at ambient temperature of (a) c-Ag_2SeO_4 and (b) glass, and smoothed data of c-Ag_2SeO_4.

pair. For normalization of the experimental data, we used the fact that, according to the definition of equation (1), $S(Q)$ approaches unity as $Q \to \infty$.

The structure factors, $S(Q)$, of glassy $0.48(AgI)_2{\cdot}0.52Ag_2SeO_4$ and of c-Ag_2SeO_4 are reproduced in figures 1 and 2(a), respectively, and figure 2(b) gives a slightly smoothed $S(Q)$ for c-Ag_2SeO_4. Despite the high AgI content of the glass, the structure of the glass is dominated by features already present in c-Ag_2SeO_4. The positions of the peaks along with those in α-AgI [28] are given in table 1.

X-ray diffraction measurements on powder samples of our c-Ag_2SeO_4 material were in full agreement with previous work [25]. The structure of c-Ag_2SeO_4 is orthorhombic with a space group $Fddd$–D_{2h}^{24}. The unit-cell dimensions at 298 K (see also references [29, 30]) are $a = 10.388$ Å, $b = 12.981$ Å, and $c = 6.050$ Å. The structure of silver selenate is isomorphic with the thernadite structure of Na_2SO_4(V) shown in figure 3 [31]. The exact Ag^+ positions in c-Ag_2SeO_4 are not specified. Taking into account the ionic radii, which are roughly 2.4 Å for the selenate (assuming a spherical approximation of the tetrahedrally shaped SeO_4^{2-} unit) and 1.13 Å to 1.26 Å for the silver ions [32], the unit cell of silver selenate is much more densely packed than is implied by figure 3.

The most pronounced difference between the two structure factors occurs at very low Q where no Bragg peak is seen for c-Ag_2SeO_4 [33] while the glass shows a VLQP at

Table 1. Summary of peak positions in the structure factors discussed in the text. In the case of c-Ag_2SeO_4 and the partly crystallized glass, the values given refer to the smoothed data. The indices 's' and 'b' stand for 'shoulder' and 'broad peak', respectively. The error in the peak positions is ± 0.02 Å^{-1}.

	c-Ag_2SeO_4 $x = 0$	Glass $x = 0.40$	Glass $x = 0.48$	Partly crystallized $x = 0.48$	Melt $x = 0.48$	Glass $x = 0.54$	α-AgI [28] $x = 1$
T/K:	298	298	298	373	573	298	573 K
No	Q_i (Å^{-1})	Q_i (Å^{-1})	Q_i (Å^{-1})	Q_i (Å^{-1})	Q_i (Å^{-1})	Q_i (Å^{-1})	Q_i (Å^{-1})
1	1.29^{s}	0.79	0.74	1.21	0.81	0.71	1.0^{s}
2	2.14	2.14	2.14	2.21	2.2^{b}	2.14	2.5
3a			3.0^{b}		2.96	3.0^{b}	2.9
3b	3.35	3.34	3.36	3.42	3.26	3.34	
4	4.61	4.5^{s}	4.5^{s}	4.52	4.5^{s}	4.5^{s}	4.4^{s}
5a		5.2			5.09		5.0
5b			5.26	5.30		5.26	5.46^{s}
5c	5.61						

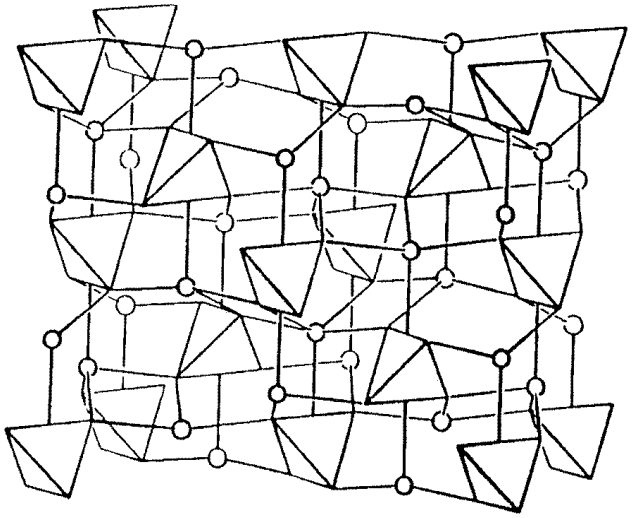

Figure 3. Orthorhombic unit cell of crystalline thernadite Na_2SO_4(V) [31], which is isomorphic with Ag_2SeO_4. The tetrahedra represent the SO_4^{2-} units, the circles the Na^+ ions.

$Q_1 = 0.74$ Å^{-1}. The value of Q_1 decreases linearly with increasing AgI content. The corresponding correlation length, $d_1 = 2\pi/Q_1$ (being approximately 8.5 Å), is about twice the ionic diameters of I^- and SeO_4^{2-} (4.4 Å and 4.8 Å, respectively). Based on the value of Q_1 and its variation with AgI content, the VLQP can be attributed to a spacing of SeO_4^{2-} units separated from each other by I^- ions.

The strongest peak for c-Ag_2SeO_4 at $Q = 2.14$ Å^{-1} ($d = 2.93$ Å) corresponds to the (311) plane which correlates positions of different silver ions, of silver and selenate ions, as well as of SeO_4^{2-} tetrahedra with different orientations (see figure 3). The two neighbouring Bragg peaks ($Q = 1.94$ Å^{-1}, $d = 3.25$ Å, (040) and $Q = 2.29$ Å^{-1}, $d = 2.74$ Å, (022)) correlate positions of Se–Se, Ag–Ag, and Ag–Se atom pairs. In both cases, the

Table 2. Weighting factors for all atom pair combinations in c-Ag_2SeO_4. W_{ij}(n) refers to neutron scattering and W_{ij}(x) to x-ray scattering.

Atom pair:	Ag–Ag	Se–Se	O–O	Ag–Se	Ag–O	Se–O
W_{ij}(n)	0.076	0.034	0.291	0.102	0.297	0.200
W_{ij}(x)	0.33	0.05	0.05	0.24	0.24	0.09
W_{ij}(n)/W_{ij}(x)	0.23	0.68	5.82	0.43	1.24	2.22

intensity is lower in the neutron than in the x-ray data, the ratio I_n/I_x being roughly 0.7 and 0.4, respectively. For this comparison, the intensities of the x-ray and neutron diffraction patterns were normalized to the strongest peak in both patterns, (311). This is in agreement with the weighting factors of the specified atom pairs given in table 2. From the strong similarity of the smoothed structure factors of c-Ag_2SeO_4 and the glass in this Q-range, the positions and orientations of the selenate units in the two materials must be similar. Swenson *et al* [8] reported significant inhomogeneities in the distribution of the refractory metals in AgI containing molybdate and tungstate glasses. On the basis of RMC simulations, they concluded that a significant degree of orientational order exists in regions with higher refractory metal (and corresponding oxygen) density while less ordering is reported in regions with lower density and more O–Ag–I–Ag–O bridges. At higher Q, the structure factors of the crystal and glass are generally similar. Deviations occur between 5 $Å^{-1}$ and 6 $Å^{-1}$, where the crystal has Bragg peaks at around 5.6 $Å^{-1}$ while the glass peak is at 5.2 $Å^{-1}$, which is closer to a value reported for α-AgI [28]. Calculations [34] based on Parrinello effective pair potentials show maxima at around 5 $Å^{-1}$ in the iodide partial structure factors of α-AgI.

Figure 4 shows the structure factors of $0.48(AgI)_2{\cdot}0.52Ag_2SeO_4$ at room temperature (glass), at 373 K and 335 K (partially crystallized material), and at 573 K (melt). Partial crystallization of the previously amorphous material starts roughly at 330 K. The $S(Q)$ show Bragg peaks at 0.7 $Å^{-1}$(with a low intensity) and at 1.01 $Å^{-1}$ (intense), and additional peaks whose positions deviate from those of pure c-Ag_2SeO_4. On heating further, the intensity of the Bragg peaks changes and additional Bragg peaks emerge. Also at 373 K, the partially crystallized material shows Bragg peaks whose positions are different from those of c-Ag_2SeO_4 as well as peaks at 0.81 $Å^{-1}$, 0.94 $Å^{-1}$, and 1.01 $Å^{-1}$, where c-Ag_2SeO_4 has none. The 0.81 $Å^{-1}$ peak corresponds to the VLQP observed in the glasses, and can, therefore, also be attributed to a distance between selenate ions. On the other hand, the structure factor of α-AgI features a shoulder at around 1 $Å^{-1}$, suggesting that, for the partially crystallized material, the peaks at 0.94 $Å^{-1}$ and 1.01 $Å^{-1}$ are related to correlations between silver and iodide ions: since the Ag–I distance is about 2.8 Å in various modifications of c-AgI [35], the Ag–Ag and I–I distances can be expected to be about 6 Å in the AgI-rich regions. From the differences between the structure factors of the partly crystallized materials and c-Ag_2SeO_4, it can be concluded that two crystalline regions form during heating, one richer in Ag_2SeO_4 and the other in AgI. This is consistent with DTA results which indicate that two exothermic processes occur at 333 K and 345 K. Further studies are needed to identify the crystalline regions formed on heating the glasses. So far, nothing is known about the phase diagram of the binary system silver iodide/silver selenate.

The presence of a VLQP at 0.81 $Å^{-1}$ in the melt at 260 K above T_g indicates that the IRO survives the melting process but its position shifts slightly to higher values corresponding to a decrease in the correlation length in the melt, which in this case is at 260 K above

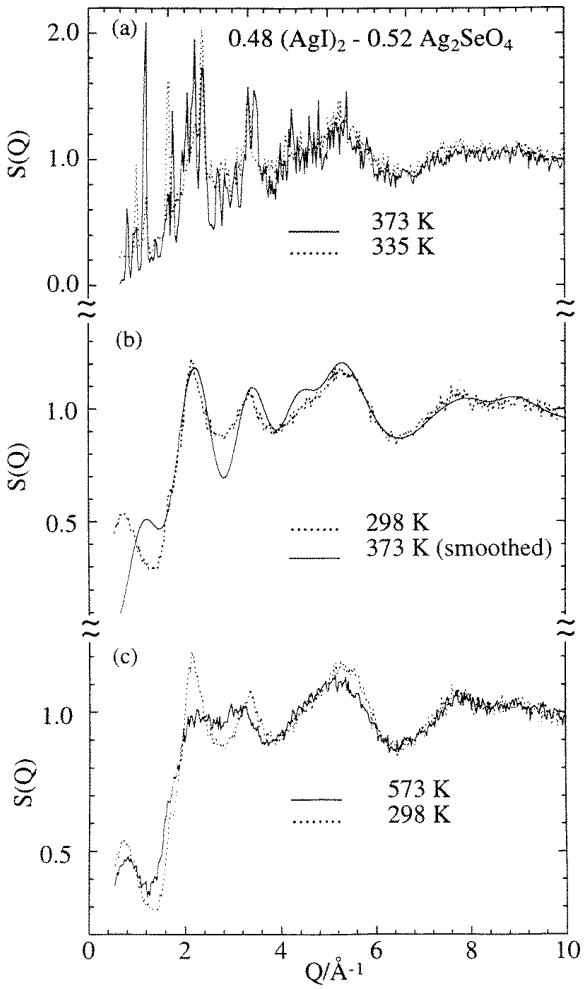

Figure 4. Structure factors of $0.48(AgI)_2 \cdot 0.52Ag_2SeO_4$: (a) partly crystallized material at 373 K and 335 K; (b) smoothed 373 K data and room temperature glass; and (c) melt at 573 K and room temperature glass.

T_g. From neutron diffraction data on $0.5AgI \cdot 0.5AgPO_3$ glass, Matic *et al* [36] reported no changes of the VLQP up to 50 K above T_g. However, Raman measurements show a partial decrease in IRO of the melt relative to the glass in the case of the alkali silicate and germanate glasses [37]. Börjesson *et al* [5–7] have suggested that the VLQP in phosphate and borate glasses is caused by density fluctuations in the phosphate or borate network rather than by structural features associated with the AgI itself. Similarly, our data suggest that the VLQP can be attributed to an average distance between the selenate ions which are kept apart by iodide ions: both silver and iodide ions push the oxygen-containing selenate units apart and the distances between them increase with AgI content. An important difference here, however, is that the selenate-containing glasses lack an underlying condensed oxide network.

The peak at 2.14 $Å^{-1}$ is much broader and less intense in the melt than in the glass or in the partially crystallized glass. As mentioned earlier, this peak, like the strongest Bragg

peak for c-Ag_2SeO_4, can be attributed to correlations between different silver ions, between Ag^+ and SeO_4^{2-} ions, and also between neighbouring selenate ions. Orientational order of the selenate ions, which may still be present in the glasses, will be lost in the melt, while the ion positions are less well defined than in the glass, and the peak broadens in both Q-directions.

At higher Q, the structure factors of the glass, partially crystallized material, and melt are generally similar. Again, deviations occur between 5 $Å^{-1}$ and 6 $Å^{-1}$ where the peaks for the glass and partially crystallized material at 5.2 $Å^{-1}$ are replaced by one peak at 5 $Å^{-1}$. This suggests that the iodide environment in the melt resembles α-AgI more than the glass does. For Q higher than 6 $Å^{-1}$ the structure factors of the glass and melt are almost identical, and the oscillations can be attributed to the Se–O distance, indicating that the SeO_4^{2-} units are present in the melt.

Table 3. Distances, r, and coordination numbers, n, of c-Ag_2SeO_4 (the line with index c) and different glasses obtained from fits to $T(r)$ described in the text. The line labelled with index t gives theoretical values for c-Ag_2SeO_4 derived from the crystal structure and the distance r_{Se-O} in this line refers to c-Na_2SeO_4 [38]. The [O–O] distances have been calculated assuming a regular tetrahedral symmetry for SeO_4^{2-}.

		Se–O			Ag–O		
x	T (K)	r (Å)	n_{Se}^{O}	n_{O}^{Se}	r (Å)	n_{Ag}^{O}	n_{O}^{Ag}
0.0[c]	298 K	1.654	3.9 ± 0.1	1.0 ± 0.1	2.35 ± 0.02	1.9 ± 0.1	0.9 ± 0.1
0.0[t]	298 K	1.654	4	1	—	2	1
0.48	298 K	1.66 ± 0.01	3.7 ± 0.2	0.9 ± 0.2	2.32 ± 0.02	0.9 ± 0.2	0.9 ± 0.2
0.48	373 K	1.65 ± 0.01	4.1 ± 0.2	1.1 ± 0.2	2.33 ± 0.01	0.9 ± 0.2	0.8 ± 0.2
0.48	573 K	1.67 ± 0.01	3.7 ± 0.2	0.9 ± 0.2	2.28 ± 0.03	1.0 ± 0.2	1.0 ± 0.2
0.40	298 K	1.66 ± 0.01	3.6 ± 0.2	0.9 ± 0.2	2.32 ± 0.01	1.0 ± 0.2	0.8 ± 0.2
0.54	298 K	1.66 ± 0.01	3.7 ± 0.2	0.9 ± 0.2	2.34 ± 0.03	0.8 ± 0.2	0.9 ± 0.2

		Ag–O			Ag–O		
x	T (K)	r (Å)	n_{Ag}^{O}	n_{O}^{Ag}	r (Å)	n_{Ag}^{O}	n_{O}^{Ag}
0.0[c]	298 K	2.48 ± 0.03	1.9 ± 0.1	0.9 ± 0.1	2.67 ± 0.01	1.9 ± 0.1	1.0 ± 0.1
0.0[t]	298 K	—	2	1	—	2	1
0.48	298 K	2.50 ± 0.03	0.9 ± 0.2	0.9 ± 0.2	2.66 ± 0.01	0.9 ± 0.2	0.9 ± 0.2
0.48	373 K	2.51 ± 0.01	0.9 ± 0.2	0.9 ± 0.2	2.64 ± 0.01	0.9 ± 0.2	0.8 ± 0.2
0.48	573 K	2.51 ± 0.01	1.0 ± 0.2	1.0 ± 0.2	2.65 ± 0.01	1.0 ± 0.2	1.0 ± 0.2
0.40	298 K	2.53 ± 0.02	1.0 ± 0.2	0.8 ± 0.2	2.62 ± 0.01	1.0 ± 0.2	0.8 ± 0.2
0.54	298 K	2.45 ± 0.03	0.8 ± 0.2	0.9 ± 0.2	2.66 ± 0.01	0.8 ± 0.2	0.9 ± 0.2

		O–O	[O–O]		Ag–I		
x	T (K)	r (Å)	r (Å)	n_{O}^{O}	r (Å)	n_{Ag}^{I}	n_{I}^{Ag}
0.0[c]	298 K	2.75 ± 0.01	2.70 ± 0.04	2.9 ± 0.1	—	—	—
0.0[t]	298 K	—	—	3	—	—	—
0.48	298 K	2.74 ± 0.03	2.71 ± 0.04	3.0 ± 0.2	2.95 ± 0.05	2.5 ± 0.3	5.2 ± 0.5
0.48	373 K	2.77 ± 0.03	2.70 ± 0.04	2.9 ± 0.2	2.98 ± 0.05	2.2 ± 0.5	4.6 ± 0.5
0.48	573 K	2.78 ± 0.01	2.73 ± 0.04	2.8 ± 0.2	2.94 ± 0.05	2.0 ± 0.2	4.2 ± 0.5
0.40	298 K	2.75 ± 0.03	2.71 ± 0.04	2.7 ± 0.2	2.92 ± 0.05	2.4 ± 0.2	6.1 ± 0.6
0.54	298 K	2.75 ± 0.02	2.71 ± 0.04	2.7 ± 0.2	2.95 ± 0.05	2.9 ± 0.2	5.2 ± 0.3

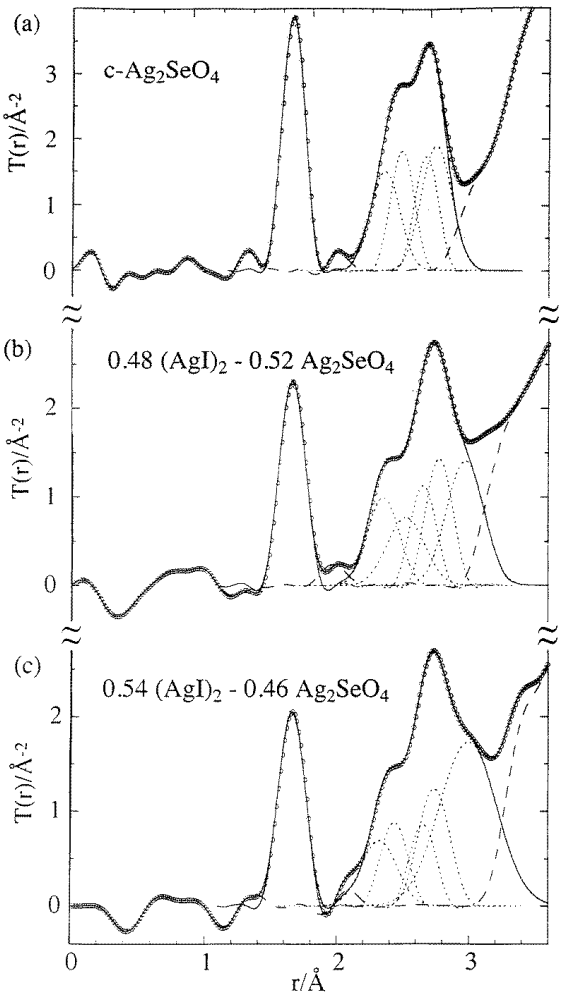

Figure 5. Here we show total pair correlation functions of the following glasses: (a) c-Ag_2SeO_4; (b) $0.48(AgI)_2{\cdot}0.52Ag_2SeO_4$; (c) $0.54(AgI)_2{\cdot}0.46Ag_2SeO_4$. Key: ○: experimental data, - - - -: Gaussians used for the fits; ——: total fitted curve; – – –: residual.

3.2. Real space: the total pair correlation functions, T(r)

The total pair correlation functions, $T(r)$, are calculated from $S(Q)$ via

$$T(r) = 4\pi r\rho_0 + \frac{2}{\pi}\int_0^{Q_{max}} Q[S(Q) - 1]\sin(Qr)\ \mathrm{d}Q \tag{2}$$

where ρ_0 is the total number density. Values of Q_{max} up to 25 Å^{-1} and the Lorch modification function [38] were used for the transformation. The Lorch function sufficiently suppresses the effects of the high-Q cut-off in $S(Q)$ seen as 'side ripples' after the Fourier transformation, while at the same time it gives an acceptable broadening of the peaks in $T(r)$. Neither the positions of the peaks in $T(r)$, nor the coordination number obtained from the fits to this function, are affected by the use of the modification function, as it is also taken into account in the fitting procedure.

$T(r)$ was fitted with a sum of several Gaussian functions: the position of each corresponds to a distance between specific atomic pairs while the area is directly related to the corresponding coordination number. In the present case, structural information on the crystalline compound c-Ag_2SeO_4 was used to assign the number of such functions as well as the positions of their maxima. The functions $T(r)$ along with the fitted functions are shown in figure 5 and various parameters are grouped in table 3. Five Gaussians were used for the fit corresponding to the Se–O pair, three different Ag–O pairs, and the O–O pair within the tetrahedra. For c-Ag_2SeO_4, for which no atomic positions for the silver ions are available from the literature, our results can be compared with data for isomorphic compounds and are found to be in good agreement. The good correspondence between the O–O distance obtained from the fitting procedure and that calculated from the Se–O distance assuming a regular tetrahedral symmetry (see table 3) show that the SeO_4 tetrahedra cannot be strongly distorted. This finding is in agreement with the results on Na_2SeO_4 from reference [39] and in contrast to those from reference [30] where the silver is reported to strongly distort the sulphate tetrahedra. A similar procedure was followed for all of the samples including those not presented here; six Gaussian functions were used, the additional one being needed to treat the Ag–I pair. The values of the parameters are listed in table 3. Figures 5(b) and 5(c) show the results of the fits to $T(r)$ for the $0.48(AgI)_2{\cdot}0.52Ag_2SeO_4$ glass and the $0.54(AgI)_2{\cdot}0.46Ag_2SeO_4$ glass, both at ambient temperature. The Se–O distances thus deduced are: 1.66 Å in all of the glasses, 1.65 Å in the partly crystallized state, and 1.67 Å in the melt, all within ± 0.01 Å. The coordination numbers of the SeO_4^{2-} units as well as the Ag–O distances are, within experimental error, the same as in c-Ag_2SeO_4. The Ag–I distance is 2.9 ± 0.1 Å, similar to that reported for the various modifications of c-AgI.

In $x(AgI)_2{\cdot}(1-x)Ag_2SeO_4$, for each Ag–O distance, the coordination number of Ag–O, $n_{Ag}^{O} \approx 1$ and—as expected—it decreases with increasing AgI content within experimental errors. For $x = 0.48$, $n_{Ag}^{O} = 0.9 \pm 0.2$ and 1.0 ± 0.2 at room temperature and in the melt, respectively, indicating a possible small increase with temperature. The Ag–I coordination numbers are less certain, with an error up to ± 0.6. In the different glasses, one silver atom is surrounded by $n_{Ag}^{I} = 2.0$ to 2.9 iodide atoms, n_{Ag}^{I} increasing with AgI content, while every iodide ion 'sees' an average of $n_{I}^{Ag} = 4.2$ to 6.1 silver atoms, decreasing with increasing AgI content. Both coordination numbers seem to decrease with increasing temperature. We find that for $x = 0.48$, $n_{Ag}^{I} = 2.5$ and 2.0 and $n_{I}^{Ag} = 5.2$ and 4.2 at room temperature and in the melt, respectively. The coordination numbers are somewhat different from those expected from the coordination numbers of the crystalline AgI phases: in the case of the cubic phases α-AgI [40] and γ-AgI, $n_{Ag}^{I} = 4$, and in the hexagonal β-phase, where two slightly different Ag–I distances exist, the corresponding coordination number is $3 + 1$. Taking into account the fact that in glasses, roughly half of the iodide ions are replaced by selenate ions, one would expect that a silver ion is surrounded by approximately two iodide ions on average. This value is close to the value found for the melt but lower than that found in the glasses, implying that for these the Ag–I environment is different from that of α-AgI.

The glass structure can be formally constructed from the Ag_2SeO_4 lattice by replacing x SeO_4^{2-} ions by $2x$ iodide ions. Our results support a process in which one half of the iodide ions replace the vacated SeO_4^{2-} ions, the ionic radius of I^- (2.2 Å) being very similar to that of SeO_4^{2-} (2.4 Å), while the other half occupy the vacant tetrahedral sites of the face-centred orthorhombic lattice. Although the ionic radii of the selenate and the iodide ions are similar, they are not identical. At the same time, the total number of ions per unit cell is changed if one selenate ion is replaced by two iodide ions. This would not only change the symmetry

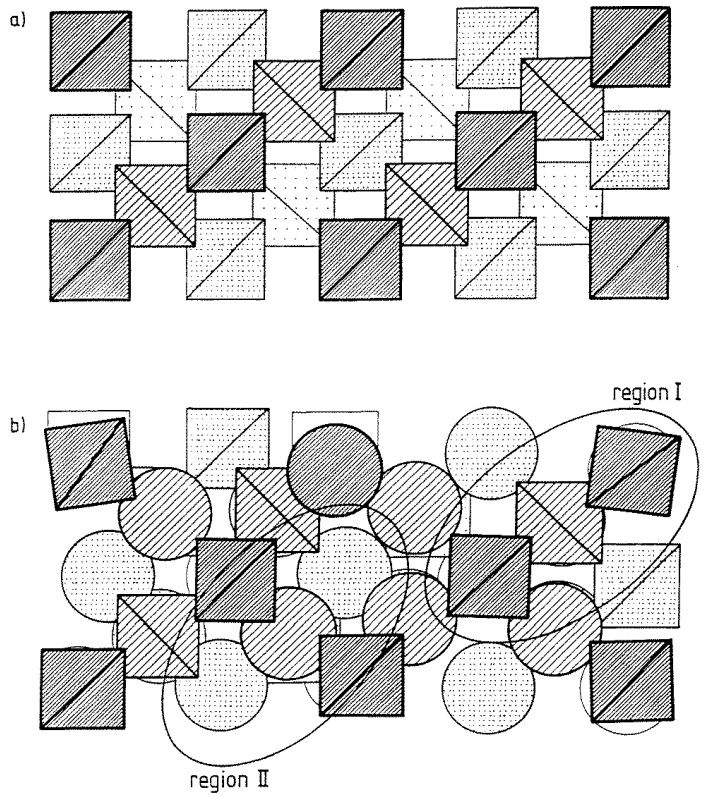

Figure 6. Schematic drawing of the structure of (a) c-Ag_2SeO_4 and (b) $x(AgI)_2{\cdot}(1-x)Ag_2SeO_4$, showing the regions I and II discussed in the conclusions. (a) shows the selenate tetrahedra of c-Ag_2SeO_4 in a projection onto the x, y plane. Tetrahedra at different z-coordinates are represented by different patterns: dense hatching: $z = 0$; light hatching: $z = c/4$; dense dotting: $z = c/2$; light dotting: $z = 3c/4$. In (b), iodide ions are represented by circles. Blank symbols correspond to $z = c$ in the crystal.

of the cell, but also increase the Coulombic forces between the now more densely packed anions. Both facts lead to a distortion of the former unit cell which results in a loss of the long-range order of the lattice, but the short-range order is maintained. This mechanism is consistent with the upper limit of the glass formation region in these glasses at $x = 0.54$, which is close to the composition value ($x = 0.5$) for which all of the vacant tetrahedral sites of the face-centred orthorhombic lattice would be occupied. It also explains why the orientational correlations of two neighbouring selenate ions are present in regions I of the structure where pairs of selenate ions exist at distances similar to those in c-Ag_2SeO_4. In other regions (II), the selenate ions are separated from each other by iodide ions creating an IRO characterized by the VLQP in the structure of the glasses and the melt. The two regions are schematically represented in figure 6. Although iodide ions are involved in the presence of the IRO, there is no evidence of formation of a biphasic structure with AgI clusters.

The partly crystallized glasses consist of a glassy matrix with two kinds of embedded crystalline region. In the molten state, all of the ions are so mobile that the relative orientations of two neighbouring selenate ions will fluctuate. The relative distances between

two selenium atoms in a configuration SeO_4^{2-}–I^-–SeO_4^{2-}, however, remain similar to that in the glass: consequently two types of region continue to exist, and so the VLQP survives the melting process.

4. Conclusions

Along with other fast-ion-conducting glasses containing AgI, silver iodide/silver selenate glasses exhibit a VLQP at $Q \approx 0.75$ Å^{-1} which is attributed to correlations between SeO_4^{2-} units separated by I^- ions. On heating, the glasses become partly crystalline, showing a Bragg peak at $Q \approx 0.8$ Å^{-1}. The VLQP survives further heating into the liquid phase.

The most pronounced structural feature in the glass is a strong peak at $Q = 2.14$ Å^{-1} which is attributed to correlations between pairs of Ag^+ ions and Ag^+ and SeO_4^{2-} units, and orientational correlations between pairs of SeO_4^{2-} tetrahedra. This feature is also pronounced in the smoothed structure factor of the partly crystalline material, but much weaker in the melt due to a loss of orientational order.

The average coordination of the Ag^+ consists of about three O atoms (at different distances) and two to three I atoms in the glasses versus two I atoms in the melt. These can be compared with an Ag–O coordination number of 6 (at different distances) in c-Ag_2SeO_4 and an Ag–I coordination number of 4 in the cubic phases of c-AgI.

Our results support a picture of two regions in the glass, as schematically illustrated in figure 6. Regions I are characterized by strong orientational correlations between neighbouring SeO_4^{2-} ions which have the same separation as in c-Ag_2SeO_4, and regions II are characterized by positional correlations with a length scale of the order of the sum of the I^- and SeO_4^{2-} ionic diameters, giving rise to the VLQP. The partly crystallized material consists of a glassy matrix embedding the two types of crystalline regions. On melting, the orientational correlations between neighbouring SeO_4^{2-} ions are reduced, but the strong positional correlations between I^- and SeO_4^{2-} persist maintaining the IRO and the VLQP. Although the iodide ions are involved in the IRO, there is no evidence of formation of biphasic structure with AgI clusters, as was proposed in some fast-ion-conducting glasses.

In addition, our results support and illuminate the findings deduced from the dynamic conductivity spectra [24]. The conductivity data revealed the existence of two kinds of ionic site: 'good sites' where an ion stays for a while once it has hopped into it, and 'bad sites' from which the ion immediately jumps back into its starting position. Bad sites cause localized ionic motion, whereas good sites contribute to the long-range ion transport. In [24] it was pointed out that favourable silver sites will be more likely to be found in the vicinity of iodide ions, whereas less favourable sites will dominate in the vicinity of selenate ions. Taking into account the neutron diffraction data presented here, we can conclude that the long-range ion transport (seen as the so-called dc conductivity) will basically occur along structural regions of type II, whereas localized ionic hopping motions are more likely to be found in regions of type I.

Acknowledgments

We would like to thank M Buscher, J Kellers, I Niederhausen, K Suzuya, D Wilmer, and especially K Funke for many interesting discussions. The crystalline silver selenate used in the glass preparation was synthesized by M Buscher. We owe special thanks to K J Volin and the IPNS staff for assistance in performing the experiments on the GLAD diffractometer. The work at ANL was supported by the US Department of Energy, Division of Materials

Science, Office of Basic Energy Sciences, under Contract W-31-109-ENG-38. CC gratefully acknowledges a fellowship from the Heinrich Hertz Foundation, Germany.

References

[1] Tachez M, Mercier R, Malugani J P and Chieux P 1987 *Solid State Ion.* **25** 263
[2] Börjesson L, Torell L and Howells W S 1989 *Phil. Mag.* B **59** 105
[3] Rousselot C, Tachez M, Malugani J P, Mercier R and Chieux P 1991 *Solid State Ion.* **44** 151
[4] Cervinka L and Rocca F 1995 *J. Non-Cryst. Solids* **192+193** 125
[5] Börjesson L, McGreevy R L and Wicks J 1992 *J. Physique Coll. Suppl.* IV **2** C2 107
[6] Börjesson L, McGreevy R L and Wicks J 1995 *Phys. Scr.* T **57** 127
[7] Swenson J, Börjesson L and Howells W S 1995 *Phys. Scr*. T **57** 117
[8] Swenson J, McGreevy R L, Börjesson L, Wicks J D and Howells W S 1996 *J. Phys.: Condens. Matter* **8** 3545
[9] Rousselot C, Malugani J P, Mercier R, Tachez M, Chieux P, Pappin A J and Ingram M D 1995 *Solid State Ion.* **78** 211
[10] Moss S C and Price D L 1985 *Physics of Disordered Materials* ed D Adler, H Fritsche and S R Ovshinky (New York: Plenum) p 77
[11] Price D L, Moss S C, Reijers R, Saboungi M-L and Susman S 1988 *J. Phys. C: Solid State Phys.* **21** L1069
[12] Wright A C, Sinclair R N and Leadbetter A J 1985 *J. Non-Cryst. Solids* **71** 295
[13] Price D L, Susman S and Wright A C 1987 *J. Non-Cryst. Solids* **97+98** 167
[14] Steeb S and Lamparter P 1984 *J. Non-Cryst. Solids* **61+62** 237
[15] Price D L 1996 *Curr. Opinion Solid State Mater. Sci.* **572–577** 1359
[16] Ellison A J G, Price D L, Dickinson J E and Hannon A C 1995 *J. Phys. Chem.* **102** 9647
[17] Armand P, Beno M, Ellison A J G, Knapp G S, Price D L and Saboungi M-L 1995 *Europhys. Lett.* **29** 549
[18] Price D L and Saboungi M-L 1998 *Local Structure from Diffraction* ed S J L Billinge and M F Thorpe (New York: Plenum) at press
[19] Kunze D 1973 *Fast-Ion Transport in Solids, Solid State Batteries Devices (Proc. NATO ASI)* ed W Van Gool (Amsterdam: North-Holland) p 401
[20] Minami T, Kazuhiro I and Tanaka M 1980 *J. Non-Cryst. Solids* **42** 469
[21] Rao K J 1987 *Rev. Solid State Sci.* **1** 55
[22] Shastry M C and Rao K J 1990 *Proc. Indian Acad. Sci. Chem. Sci.* **102** 541
[23] Frebel D 1995 *Diploma Thesis* Münster University
[24] Cramer C and Buscher M 1998 *Solid State Ion.* **105** 109
[25] *Powder Diffraction File* 1993 NBS Monogram 25, vol 2 (Washington, DC: US Government Printing Office) p 32
[26] Price D L 1987 Intense pulsed neutron source *Argonne National Laboratory, Note* No 19
[27] Howe M A, McGreevy R L and Howells W S 1989 *J. Phys.: Condens. Matter* **1** 3433
[28] Howe M A, McGreevy R L and Mitchell E W J 1985 *Z. Phys.* B **62** 15
[29] In contrast to
Landolt–Börnstein New Series 1982 vol 7 (Berlin: Springer) p 343
and the *Powder Diffraction File* based on reference [25], where the unit-cell lengths of c-Ag_2SeO_4 are specified as $a = 10.388$ Å, $b = 12.981$ Å, and $c = 6.050$ Å (298 K), the *Structural Reports* give the following data: $a = 6.069$ Å, $b = 12.815$ Å, and $c = 10.211$ Å. The latter values are taken from the older reference [30].
[30] Herrmann K and Ilge W 1931 *Z. Kristallogr.* **80** 402
Zachariasen W H 1932 *Z. Kristallogr.* **82** 161
[31] *Strukturberichte (Structural Reports)* 1937 vol 2 (Leipzig: Akademische) p 89
[32] *Landolt–Börnstein Series* 1955 vol 1 (Berlin: Springer) pp 523–5
[33] Like for the glasses, the $S(Q)$ of c-Ag_2SeO_4 has been experimentally determined down to a lowest Q-value of 0.5 Å^{-1}. The $S(Q)$ of c-Ag_2SeO_4 is approximately 0 for $Q < 1$ Å^{-1}. All of the low-Q data are included in figure 2.
[34] Stafford A J and Silbert M 1987 *Z. Phys.* B **67** 31
[35] This is true for the two room temperature phases, β- and γ-AgI, as well as for the high-temperature phase, α-AgI; see e.g.:
Gmelin Handbuch der anorganischen Chemie 1972 61st edn, vol B2 (Weinheim: Chemie) p 215 ff
[36] Matic A, Börjesson L, Wannberg A and McGreevy R L 1996 *Solid State Ion.* **86–88** 421

[37] Sharma S K, Cooney T F and Wang S Y 1994 *J. Non-Cryst. Solids* **179** 125
[38] Lorch E 1969 *J. Phys. C: Solid State Phys.* **2** 229
[39] Kalman A and Cruickshank D W J 1979 *Acta Crystallogr.* B **26** 436
[40] From their x-ray diffraction data on α-AgI, Strock [41] and Hoshino [42] deduced an average distribution of the silver ions over a large number of sites. Newer neutron diffraction results on an α-AgI single crystal by Cava *et al* [43], however, clearly indicated that the nuclei of the silver ions are found in elongated ellipsoidal regions, the equilibrium position being the tetrahedral site.
[41] Strock L W 1934 *Z. Phys. Chem.* B **25** 411
Strock L W 1936 *Z. Phys. Chem.* B **31** 132
[42] Hoshino S 1957 *J. Phys. Soc. Japan* **12** 315
[43] Cava R J, Reidinger F and Wuensch B J 1977 *Solid State Commun.* **24** 411